Fibers and Polymers 2003, Vol.4, No.3, 102-106

Crystallization Behaviour of PP and Carbon Nanofibre Blends

A. Chatterjee and B. L. Deopura*

Department of Textile Technology, IIT Delhi, New Delhi-110016, India
(Received May 19, 2003; Revised August 6, 2003; Accepted August 13, 2003)

Abstract: Crystallization behaviour of blends of different MFI isotactic polypropylenes (PP), and blends of PP with carbon nanofibre have been investigated by DSC and polarizing optical microscope. Both higher MFI PP component and the carbon nanofibre in the blend influence the nucleation activity of the melt during non-isothermal crystallization. In presence of carbon nanofibre, the sherulitic growth rate is highly disturbed. The calculation of nucleation activity indicates that carbon nanofibres act as active substrate for heterogeneous nucleation.

Keywords: Polypropylene, Carbon nanofibre, Crystallisation kinetics, Nucleation activity, Spherulites

Introduction

There is an increasing demand for novel polymeric material with improved physical properties for high tech applications. Blending of polymers and polymer composites are two important approaches towards achieving novel polymeric material. More recently, the advantages of using polymer mixtures have become so apparent that almost one third of polymer usage is in the form of blends of polymer. Considering these facts, a new approach for development of high modulus polypropylene has been thought of. In this approach, two different molecular weight PP has been blended in a range of blend ratios and processed in the conventional fibre processing method. The process was optimized in terms of modulus. Further improvement of modulus is aimed at by incorporating carbon nanofibre in the blended polymer matrix.

There are a few reports on the blends of different molecular weight polypropylenes. It has been reported that blending leads to lower impact resistance, however processability of blends was superior to that of the PP of comparable viscosity. Blends of PP resins [1] were found to have better spinning performance for fine denier fibres than those prepared from individual resins. In two different studies of blending plastic grade and fibre grade PPs, improvement in mechanical properties of the blended filaments had been reported [1,2]. The improvement was attributed to (a) increased amorphous orientation (b) the high molecular weight segment acting as tie molecules and (c) a possible reduction in the crystal sizes.

Exceptional properties of carbon nanotubes and nanofibres have led to the development of polymer nanocomposites containing nanotubes and nanofibres. Incorporation of carbon nanotubes and carbon nanofibres has been previously demonstrated to increase the physical properties of the matrix material [3-7]. The improvement in mechanical properties is most pronounced with crystalline polymers due to the action of filler particles acting as nucleation agents and thereby increasing the degree of crystallinity. It is also known that the greatest advantage of most semicrystalline polymers is their ability to self-reinforce via the formation of fibrillar structure when stretched at high temperature [8]. Thus, it is expected that the nanofibre, with their submicron diameter, could easily be incorporated in the fibrillar structure leading to superior composite material. It has been demonstrated that traditional fibre spinning technology can be used for spinning polymer/carbon nanofibre composite [8,9].

Nonisothermal crystallization studies of polymers have been widely carried out because of the analogous crystallization condition to that of real processing. Since the crystalline phase has significant effect on the mechanical and thermal properties of the polymer, the crystallization behaviour of the blend, as well as, the composite have been studied with the help of polarizing microscope and DSC techniques.

Experimental

Material

The isotactic polypropylene was provided by Reliance Industries Ltd. Two different PP samples with 3 and 35 MFI were used. The carbon nanofibre, Pyrograph-III, was provided by Applied Science Inc., USA. The polypropylene polymers were extruded in a Betol single screw extruder and subsequently drawn over hot plates. For blending, different MFI PP chips are tumble blended in different weight proportions. Master batch of 35MFI PP with carbon nanofibre was produced in a Shirley Laboratory Blender for subsequent melt mixing with polymer during extrusion.

Nucleation and spherulitic growth of 35MFI PP, 35MFI and 3MFI PP blend and PP/carbon nanofibre blend composite samples were studied by using a polarizing microscope Leika, with a Mettler hot stage. The samples were sandwiched between glass slide and microscope cover glass, heated to 190 °C, held for 5 minutes and cooled to 133 °C, the spherulitic growth was observed under isothermal condition.

The calorimetric measurements were carried out in a

*Corresponding author: bdeopura@textile.iitd.ernet.in

Perkin Elmer Pyris -1 Series differential scanning calorimeter in nitrogen atmosphere. For all experiments the sample weight was approximately 5 mg. The samples were melted at 190 °C and held at that temperature for 10 min to erase previous thermal history and then cooled at cooling rates of 5, 10, 15, and 20 °C/min. The exothermal curves of heatflow, as a function of temperature, were recorded to analyze the nonisothermal crystallization process.

Results

Nonisothermal Crystallization Analysis

Figure 1 shows the heatflow as a function of temperature curves for the 35MFI PP, 35 and 3MFI blend (90:10 weight ratio), and 35MFI, 3MFI and carbon nanofibre (89:10:1 weight ratio) blend. From these curves, the onset temperature of crystallization, T_o; the exothermic peak temperature T_p; and the end temperature of crystallization T_c have been

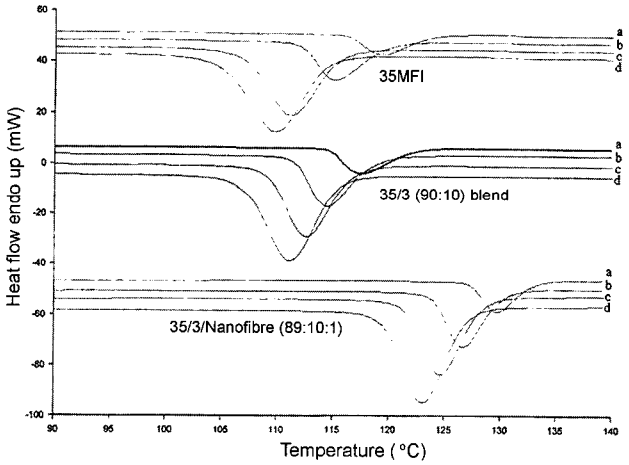

Figure 1. DSC curves of non-isothermal crystallization at different cooling rates (From a to d in increasing order of cooling rates).

Table 1. Different parameters of DSC experiment

	ϕ (°C/min)	T_o (°C)	T_p (°C)	T_c (°C)
35 MFI	5	123.8	119.3	116.3
	10	119.9	115.2	112.1
	20	115.6	111.1	107.0
	25	114.3	109.7	104.9
35/3 (90:10)	5	122.2	117.4	114.6
	10	118.6	114.4	111.5
	15	116.6	112.6	109.1
	20	115.4	111.2	106.9
35/3/NF (89:10:1)	5	132.9	129.7	127.3
	10	130.2	126.7	123.8
	15	128.4	124.6	121.4
	20	126.9	123.1	119.5

determined and are listed in Table 1. It is seen that there is no significant change in the T_o and T_p values on 10 % blending of 3MFI with 35MFI PP. But there is definite increase in the values of T_o and T_p on incorporation of 1 % nanofibre. This indicates that the rate of crystallization increases and the degree of supercooling required for crystallization reduces when nanofibres are introduced in the polymer.

To further analyze the crystallization process, the non-isothermal crystallization kinetics of 35MFI PP, 35 and 3 MFI blend, and that of the 35/3/carbon nanofibre composite sample are compared. The nonisothermal crystallization can directly be analyzed by the Avrami equation [10]:

$$X(t) = 1 - \exp(-kt^n) \quad (1)$$

Which can be written as,

$$\log[-\ln(1 - X(t))] = n\log t + \log k \quad (2)$$

Where $X(t)$ is the relative crystallinity at crystallization time t, n is the Avrami exponent, k is the crystallization rate constant. In the nonisothermal process, the crystallization time t can be determined as follows:

$$t = \frac{T_o - T}{\phi}, \text{ Where } \phi \text{ is the cooling rate.} \quad (3)$$

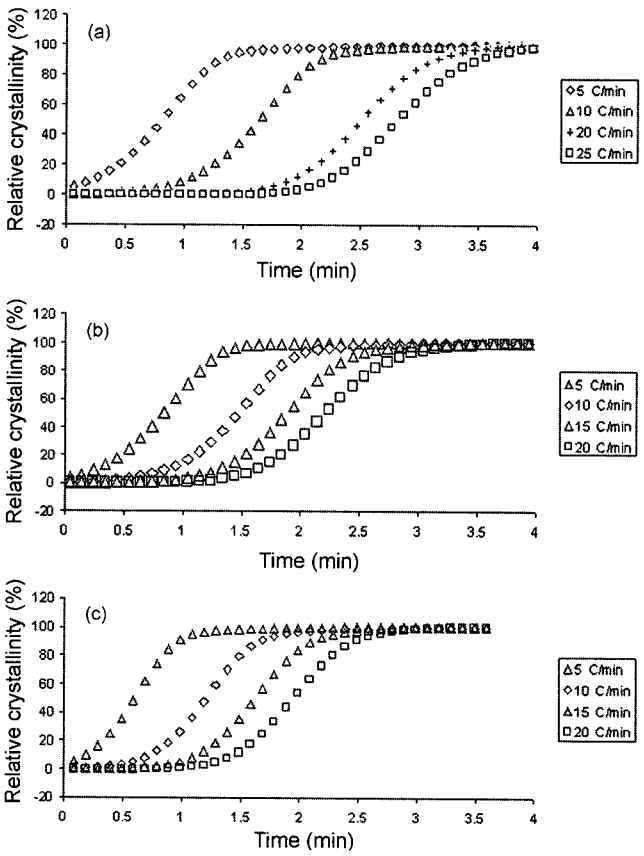

Figure 2. Relative crystallinity vs. time plots of (a) 35MFI, (b) 35/3MFI blend, and (c) 35/3/carbon nanofibre composite.

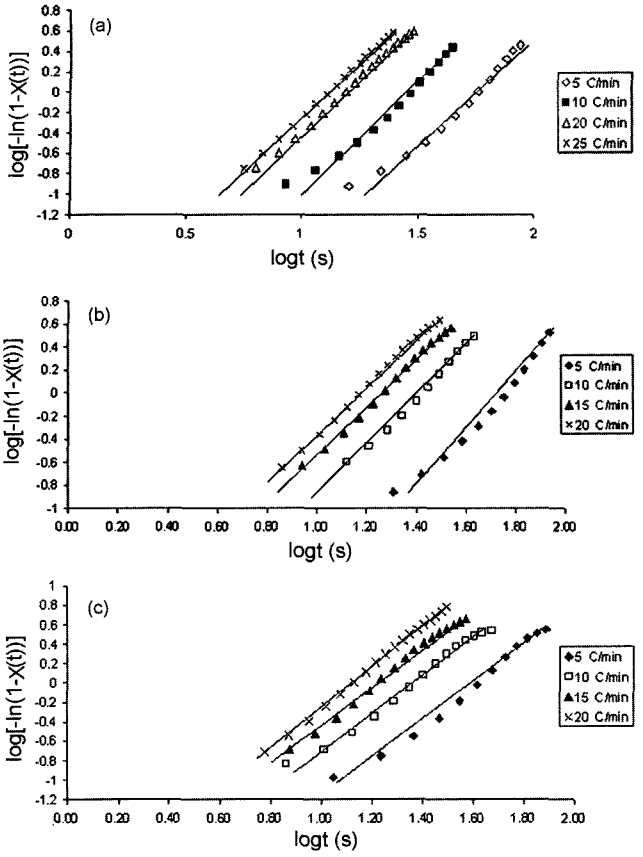

Figure 3. log[−ln(1 − $X(t)$)] vs log$t$ plots of (a) 35MFI, (b) 35/3MFI blend, and (c) 35/3/carbon nanofibre composite.

Figure 2 shows the development of relative crystallinity $X(t)$ with time t at different cooling rates for the three different samples. Plots of log[−ln(1 − $X(t)$)] vs. log$t$ are shown in Figure 3. Each curve shows only the linear portion, from which a roll-off at high relative crystallinity region was removed. Small deviations from linearity in the short-time region where logarithmic plotting tends to exaggerate small errors in the assignment of the start of the crystallization were also removed in order to show the proportional region more clearly [10]. From the slope and the intercept of the plot log [−ln(1 − $X(t)$)] vs. log$t$, the kinetic parameters n and k can be derived respectively and are given in Table 2.

Considering the influence of the various cooling rates on the nonisothermal crystallization process, Kissinger [11] suggested a method to determine the activation energy ΔE_T for the transport of the macromolecules to the growing surface from the variation of T_p with cooling rate (ϕ), which is as follows:

$$\frac{d[\ln(\phi/T_p^2)]}{d(1/T_p)} = -\frac{\Delta E_T}{R} \quad (4)$$

Where R is the gas constant. Activation Energy ΔE_T can be

Table 2. Kinetic parameters from the Avrami analysis

	ϕ (°C/min)	n	K (s^{-n})
35 MFI	5	2.16	5.011×10^{-5}
	10	2.16	5.162×10^{-4}
	20	2.00	2.511×10^{-3}
	25	2.25	3.98×10^{-3}
35/3MFI (90:10)	5	2.40	5.011×10^{-5}
	10	2.40	5.011×10^{-4}
	15	2.52	1.258×10^{-3}
	20	2.22	1.99×10^{-3}
35/3/NF (89:10:1)	5	2.25	5.162×10^{-4}
	10	2.33	1.778×10^{-3}
	15	2.16	3.162×10^{-3}
	20	2.40	3.98×10^{-3}

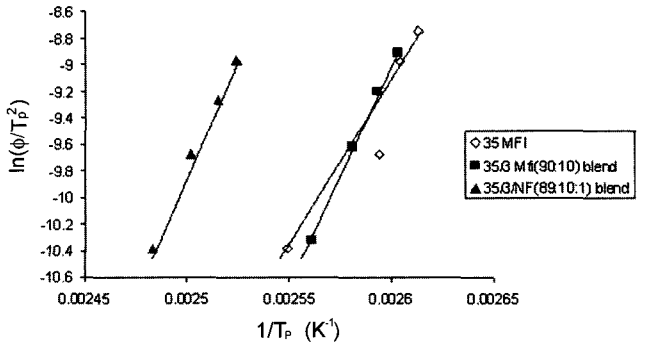

Figure 4. ln(ϕ/T_p^2) vs $1/T_p$ plots.

Table 3. Activation energy

	Activation energy (kJ/mol)
35 MFI	214.8
35/3MFI (90:10)	281.5
35/3/NF (89:10:1)	345.5

derived from the slope of the plot $\ln(\phi/T_p^2)$ vs. $1/T_p$ as shown in Figure 4. The activation energy values as calculated are given in Table 3.

The presence of nanofibre increases the activation energy (ΔE_T). In spite of the increase in the activation energy (ΔE_T), the nanocomposite exhibited increased crystallization rate and reduced degree of super cooling, as shown by the DSC data, which may be due to a change in nucleation rate. To have a better idea about the nucleation rates of the three different samples, Dobreva and Gutzow [12,13] method is used for further analysis. In case of nonisothermal crystallization process, the following relation was proposed:

$$\mathrm{Log}\,\phi \approx \mathrm{const} - \frac{B}{2.3\Delta T_p^2} \quad (5)$$

Where, ΔT_p is $T_m - T_p$, T_m is the melting temperature and B a parameter which can be calculated from the equation:

$$B = \omega \frac{\sigma^3 V_m^2}{3kT_m \Delta S_m^2 n} \quad (6)$$

Where, V_m is the molar volume of crystallizing polymer, ΔS_m is the entropy of melting, k is the Boltzman constant, σ is the specific surface energy and ω is the geometrical factor and n is the Avrami exponent. The activity of the nucleation of the filler 'ε' is defined as the ratio between the three-dimensional work of nucleation with and without filler (A_f and A_0 respectively). If the filler is extremely active for nucleation then ε approaches 0 and for absolutely inert particle, the value of ε is 1. Further, the three-dimensional work of nucleation A is equal to $nTmB$, where n is the Avrami exponent. Since the values of n are almost similar in this case so the following relation hold [10]:

$$\varepsilon = A_f/A_0 = B_f/B_0 \quad (7)$$

Thus, the nucleation activity ε can be directly calculated from the slope of the linear plots of $\log\phi$ vs $B/(2.3\Delta T_p^2)$ for the three different samples (Figure 5). The nucleation activities of the 35/3MFI blend and that of the nanocomposite are given in Table 4.

It is clearly seen that addition of 3MFI PP in 35MFI PP favours the nucleation and the carbon nanofibres further enhances the nucleation activity.

Polarised Optical Microscope Analysis

From Figure 6, it is seen that addition of 3MFI PP and carbon nanofibre increases the nucleation density, which is in accordance with our earlier analysis. The spherulitic growth rate (Figure 7) of 35MFI is more than that of 35/3MFI blend which corroborates the difference in activation energy of 35MFI and 35/3MFI blend and also matches with the earlier findings reported in the literature [1]. In case of nanocomposite, very high density of nucleation could be noticed, which grows simultaneously and covers the whole area like a cobweb and spherulitic growth rate could not be measured.

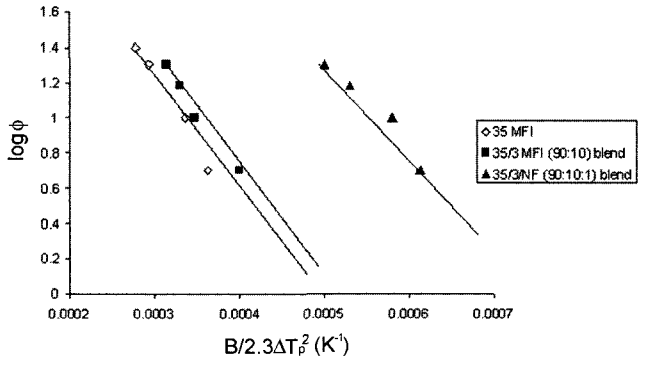

Figure 5. Plots of $\log\phi$ vs $B/(2.3\Delta T_p^2)$.

Table 4. Nucleation activity

	35/3MFI (90:10)	35/3/NF (89:10:1)
Nucleation activity (ε)	0.84	0.64

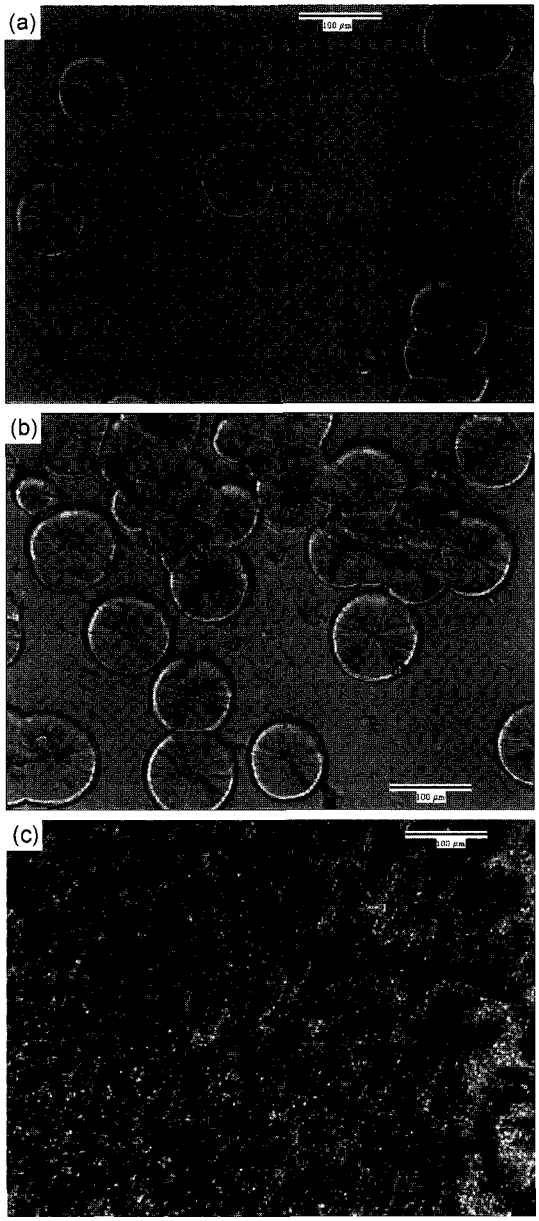

Figure 6. Selective photographs of polarized optical microscope study. (a) 35 MFI at 133 °C after 20 min., (b) 35/3 MFI (90:10) blend at 133 °C after 20 min., (c) 35/3/carbon nanofibre composite at 133 °C after 20 min.

During the crystallization of fibre reinforced polymers, fibres are shown to have a dual effect, i.e., increased nucleation and decreased spherulitic growth rates [14]. Growth of tran-

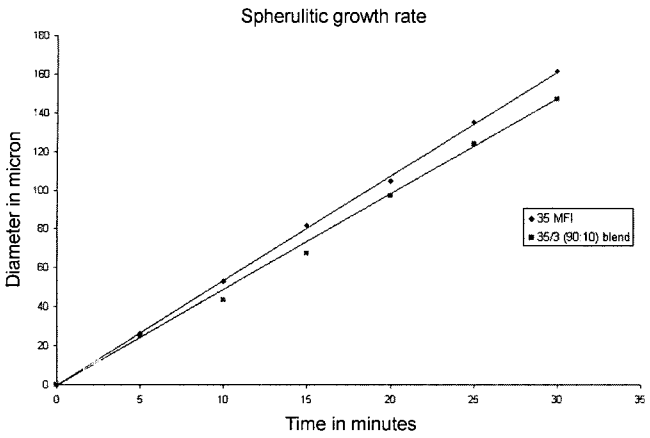

Figure 7. Spherulitic growth rate.

scrystalline zone and epitaxies are often reported. The ability of different fibres, like high modulus carbon fibre, aramid, polyethylene terepthalate and polyamide fibres, whose surfaces provide nucleation sites for PP and promote transcrystalline growth of different morphology are widely reported in literature [14-18]. But in the present study no clear transcrystalline growth was observed. The carbon nanofibres seems to be well dispersed in the melt. These dispersed fine particles/ fibres are acting as the nucleation sites.

Conclusion

Both the low MFI PP and the carbon nanofibre act as a nucleating agent for high MFI PP. The nucleating activity of the lower MFI PP and that of the carbon nanofibre towards higher MFI PP have been evaluated by the Dobreva's method. Activation energies, as calculated by the Kissinger's method, show an increase for both. Addition of carbon nanofibre decreases the spherulitic growth rate of PP.

Acknowledgement

Authors wishes to thank Dr. S. Mahajan, Reliance Industries Ltd, India and Applied Science Inc., USA for supplying the polypropylene chips and the carbon nanofibres respectively.

References

1. B. L. Deopura and S. Kadam, *J. Appl. Polym. Sci.*, **31**, 2145 (1986).
2. S. J. Mahajan, K. Bhaumik, and B. L. Deopura, *J. Appl. Polym. Sci.*, **43**, 49 (1991).
3. A. Chatterjee and B. L. Deopura, *Fiber Polym.*, **3**, 134 (2002).
4. A. K. Lau and D. Hui, *Composites, Part B*, **33**, 263 (2002).
5. E. T. Thostenson, Z. Ren, and T. W. Chou, *Compos. Sci. Technol.*, **61**, 1899 (2001).
6. K. Lozano and E. V. Barrera, *J. Appl. Polym. Sci.*, **79**, 125 (2001).
7. R. D. Patton, C. U. Pittman Jr., L. Wang, and J. R. Hill, *Compos., Part A- Appl. Sci.*, **30**, 1081 (1999).
8. S. A. Gordeyev, J. A. Ferreira, C. A. Bernardo, and I. M. Ward, *Mat. Lett.*, **51**, 32 (2001).
9. S. Kumar, H. Doshi, M. Srinivasarao, J. O. Park, and D. A. Schiraldi, *Polymer*, **43**, 1701 (2002).
10. J. Li, C. Zhou, and W. Gang, *Polym. Test.*, **22**, 217 (2003).
11. H. E. Kissinger, *J. Res. Natl. Stand.*, **57**, 217 (1956).
12. A. Dobreva and I. Gutzow, *J. Non-crystalline Solids*, **162**, 1 (1993).
13. A. Dobreva and I. Gutzow, *J. Non-crystalline Solids*, **162**, 13 (1993).
14. G. Bogoeva-Gaceva, A. Janevski, and E. Mader, *Polymer*, **42**, 4409 (2001).
15. J. L. Thomason and A. A. VanRooyen, *J. Mat. Sci.*, **27**, 889 (1992).
16. J. Verga and J. Krager-Kocsis, *J. Mat. Sci. Lett.*, **13**, 1069 (1994).
17. E. Assouline, R. Fulchiron, J.-F. Gerard, E. Wachtel, H. D. Wagner, and G. Marom, *J. Polym. Sci., Part B, Polym. Phys.*, **37**, 2534 (1999).
18. T. E. Sukhanova, F. Lednicky, J. Urban, Y. G. Baklagina, G. M. Mikhailov, and V. V. Kudryavstev, *J. Mat. Sci.*, **30**, 2201 (1995).